Calibration of Cherenkov Detectors for the Muon Ionization Cooling Experiment (MICE)

2214432

E-mail: 2214432d@student.gla.ac.uk

Abstract. Accelerator physics has made significant technological leaps in the last few decades. Muon colliders offer a specially attractive option for future high-energy colliders which can lead to new and interesting discoveries. The Muon Ionization Cooling Experiment (MICE) aims to prove the feasability of muon colliders and neutrino factories for future research by reducing the phase-space in a muon beam via ionisation cooling. This report details the calibration of Cherenkov detectors present within the MICE apparatus in order to complement the Time-Of-Flight detectors in particle identification. Data chosen to perform the calibration of the Cherenkov detectors consists of pion momentum scans in a range of 140 MeV - 400 MeV. For each pion momentum scan distinguishable peaks in time-of-flight are observed, with varying degrees of overlap between the peaks. For pion scans in a higher momentum range, there was a noticeable contamination in the pion samples due to muons. Plots of number of photoelectrons (N_{PE}) as a function of momentum p(MeV) were generated and it was observed that the muon Cherenkov threshold was lower than the pion Cherenkov threshold. Muons were found to emit a larger number of photons than pions did for the same momentum.

1. Introduction

The Muon Ionization Cooling Experiment (MICE) is a particle physics experiment being conducted at the Rutherford Laboratory in the UK. MICE aims to demonstrate the possibility of reducing the phase-space in a muon beam via ionisation cooling. The success of this experiment will be used to prove the feasability of muon colliders and neutrino factories viable for future research [1].

Muons are fundamental particles with 207 times the mass of an electron and and they are highly unstable. They decay into electrons (positrons), neutrinos and antineutrinos:

$$\mu^- \rightarrow e^- + \bar{\nu}_e + \nu_\mu \tag{1}$$

$$\mu^+ \rightarrow e^+ + \nu_e + \bar{\nu}_\mu \tag{2}$$

Muon colliders offer a specially attractive option for future high-energy colliders since muons are fundamental particles, like electrons and positrons, so all the accelerator energy can be used to create new particles, unlike the Large Hadron Collider that accelerates protons, and only about 10 percent of the energy is effectively used for the creation of new particles. Furthermore, since they have much higher mass than electrons, they can be accelerated to very high energies at a circular collider without losing energy by synchrotron radiation. Linear colliders need to be used for electron-positron colliders due to the energy loss that they would suffer due to

synchrotron radiation in a circular facility. Therefore, the reduced synchrotron radiation enables the acceleration of muons in a circular collider and their collisions [2].

MICE aims to demonstrate that it is possible to reduce the phase space of a beam of muons using ionisation cooling. Modern particle colliders that rely on stable particles for collisions cool a particle beam by using magnetic fields to modify the trajectory of the particles, such as electron cooling or stochastic cooling, in a circular storage ring. However, due to their instability, muons tend to decay too quickly (with a mean lifetime of 2.2 μs) to be cooled by this method [3].

A muon beam can be characterised by its longitudinal momentum along the direction in which the beam is travelling and its transverse momentum at right angles to the direction of travel. The transverse phase space is given by the four variables perpendicular to the direction of motion (x, p_x, y, p_y). A particle that passes through a material loses energy and its momentum is reduced in all directions. Such a beam can be accelerated by RF cavities that increase the momentum along the longitudinal beam direction. This reduces the transverse phase space of the beam, thereby creating a cooling effect. The emittance is a quantity that is proportional to the volume of phase space. MICE attempts to minimise transverse emittance using ionization cooling. The muons are made to pass through a material (typically liquid hydrogen or lithium hydride) which causes the muons to lose energy as they interact with the material. After the muons have lost energy, they are given energy back, via radio frequency electric fields, in the direction of propagation of the beam, causing the transverse size of the beam to shrink [4].

MICE also offers an opportunity for researchers to offer realistic designs for Neutrino Factories which require that intense muon beams are accelerated and stored in a muon storage ring, where they decay to create neutrino beams. A neutrino factory is used for creating neutrino beams with better intensity and flavour composition. Neutrino beams can help make new domains of physics accessible by supplying higher quality beams at longer baselines [5]. These beams will be able to elucidate properties of neutrinos, such as their mass-squared difference and mixing angles, with unprecedented accuracy and would determine whether CP is violated in neutrinos, a key to understanding the matter-antimatter asymmetry of the universe.

This report aims to show the successful calibration of Cherenkov detectors for MICE. The report is structured as follows:

- **The Muon Ionization Cooling Experiment (MICE)** section provides details of the experiment and discusses phase space measurement as well as particle identification.
- **The Calibration of Cherenkov detectors** section details how Cerenkov detectors in MICE work. Data used in this experiment is described and detailed and the method for calibration of the detectors discussed.
- **The Results** section provides plots obtained for both TOF and Cherenekov detectors.
- Finally, the **Conclusion** section provides a discussion of the most important results obtained.

2. Muon Ionization Cooling Experiment (MICE)

The Muon Ionisation Cooling Experiment (MICE) is a global collaboration of particle physicists, accelerator physicists and engineers, whose aim is to engineer and demonstrate a muon ionization cooling channel. Successful demonstration of MICE is essential for designing muon colliders or neutrino factory in the future.

The MICE apparatus can be broken down into several sections. To create the beam, protons are accelerated to 800 MeV at the ISIS accelerator facility and collide into a dense titanium target. Upon collision, the atoms within the target emit pions. Since pions are unstable, they decay into a muon and a neutrino. Since neutrinos are without charge and have negligible mass, they pass out of the experiment while charged muons are directed into

the experiment using quadrupole and dipole magnets. Muons are then made to pass through an absorber material made of liquid hydrogen or lithium hydride. The muons collide with the atoms in the absorber and lose electrons, thus the muons lose energy due to ionisation. Magnetic fields guide particles through the cooling channel, where the properties of the beam are analysed in sections present before and after the absorber, to measure ionization cooling. The incident muon beam encounters a diffuser that inserts a controlled amount of material in the beam in order to increase the emittance of the beam and make it tuneable. Accurate time measurement and particle identification are conducted by time-of-flight (TOF) detectors both upstream (TOF0 and TOF1) and downstream (TOF2) of the cooling channel. The section beyond the diffuser contains an input spectrometer consisting of scintillating-fibre tracking devices within a uniform-field superconducting solenoid that are used to measure the phase space each individual particle that passes through. Past this section lies the cooling section, with either a liquid hydrogen absorber inside a vessel or a lithium hydride (LiH) absorber inside a superconducting focus coil. Data such as the momentum and position of outgoing particles are recorded in a second spectrometer. There is another time-of-flight (TOF) detector downstream which performs additional TOF measurements and particle identification is conducted by means of a calorimeter system consisting the KL preshower detector and the Electron-Muon Ranger (EMR). To minimise emittance growth, the magnets in these two cells are matched to the spectrometer solenoids [6].

To reject background from pions and electrons, Cherenkov detectors and time-of-flight detectors are used to perform particle identification and distinguish muons from pions. A calorimeter at the end distinguishes electrons from muons [7]. The MICE cooling channel is described in Figure 1 and the full beamline and detector elements are shown in Figure 2.

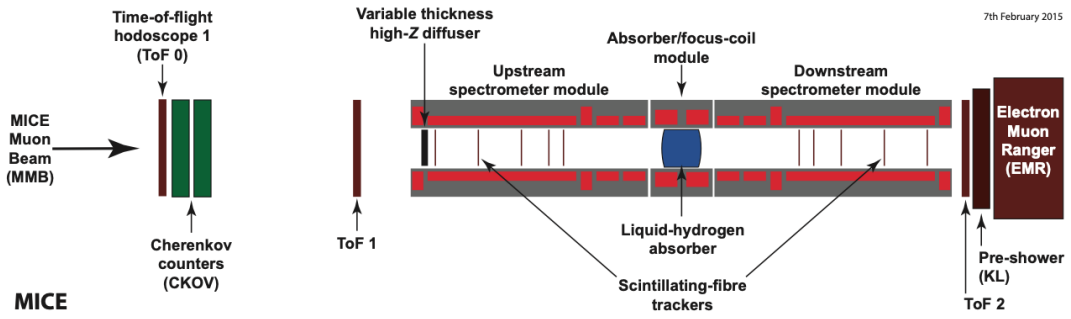

Figure 1. Schematic diagram of the MICE cooling channel [8]

In order to distinguish between particles, MICE utilises a number of particle identification detectors:

- **Time of Flight Detectors (TOF)**
  Due to the difference in mass of muons from pions and electrons, these TOF detectors are used to measure the difference in velocity between muons and other background particles [9].
- **Cherenkov detectors**
  At a higher momentum range, the difference for time of flight for muons and pions decreases significantly, making particle identification with TOF detectors quite difficult. TOF detectors are then complemented by Cherenkov detectors [10]. Cherenkov detectors work on the principle that a charged particle passing through an optically transparent

material at a velocity higher than that of light in the material emits light, known as Cherenkov radiation. This light is emitted with an angle θ such that

$$\cos\theta = \frac{c}{nv} \tag{3}$$

where c is the speed of light in a vacuum, n is the refractive index of the medium, and v is the speed of the particle. The angle θ and the number of photoelectrons emitted by each particle can thus be used to measure the speed of a particle and help in particle identification.

- **KL**
  The KLOE-Light (KL) detector is a calorimeter that uses lead layers alternating with scintillating fibers to identify particles by analysing their energies as the particles shower in the detector. Electrons have a larger probability of showering in KL and, as a result, have broader KL distributions compared to muons and pions [11].
- **EMR**
  The Electron-Muon Ranger (EMR) is used to tag muons that pass through the MICE cooling channel without decaying. The detector can identify electrons with an accuracy of 98.6%. The EMR is also used for the reconstruction of muon momentum within a range of 100 MeV/c - 280 MeV/c [11].

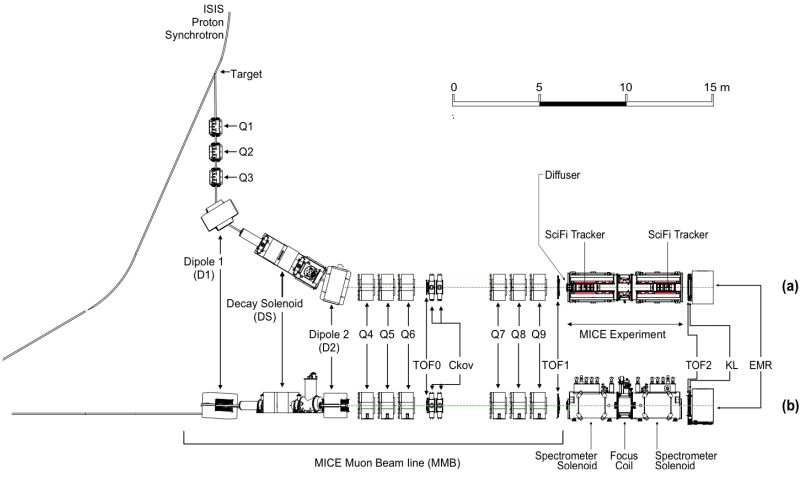

Figure 2. Schematic Diagram of the Muon Ionization Cooling Experiment [8].

3. Calibration of the Cherenkov Detectors

Data chosen to perform the calibration of the Cherenkov detectors consists of pion momentum scans in a range of 140 MeV - 400 MeV. Data was buffered in the form of ROOT files [12] containing information of the details of every particle crossing the MICE detectors for each individual spill of data from the accelerator, which operated at 50 Hz.

MICE conducts particle identification by using two Time of Flight (TOF) counters (TOF0, and TOF1) made of scintillating slabs. Electrons, with smaller masses, and pions, with larger masses, have respectively shorter and longer times of flight than muons and, as a result, they each have a distinct time-of-flight peak (Figure 3) [13].

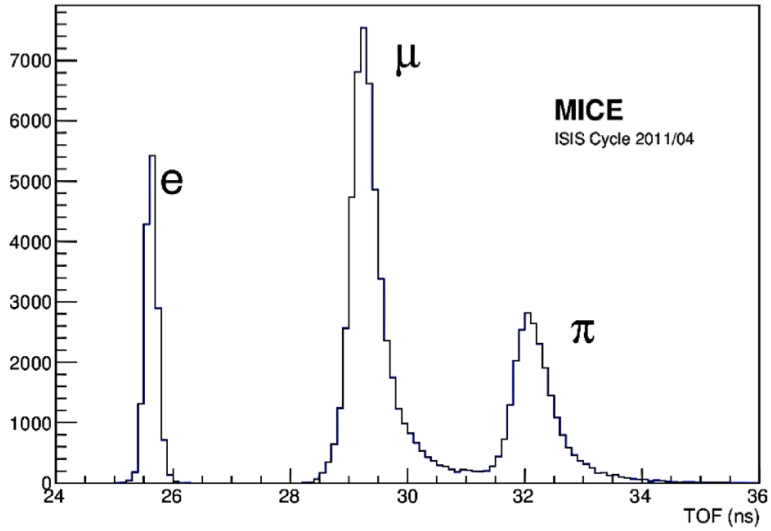

Figure 3. Example of a plot of time-of-flight (TOF) in ns between the TOF0 and TOF1 detectors for a beam corresponding to 222 MeV/c. Three distinct peaks between TOF0 and TOF1 are observed, corresponding to electrons (e), muons (μ) and pions (π) [13].

At higher momentum range (above 220 MeV/c) the difference of time-of-flight for μ and π decreases from 2.4 ns to 1 ns over 10 m distance (approximate distance between TOF0 and TOF1). This creates difficulties in μ/π separation by the TOF technique [14]. The Cherenkov detectors are used as complementary devices for particle identification and are located past TOF0 in the MICE apparatus.

Due to their differing refractive indices, CkovA and CkovB are used to reject background pions and electrons. The measured refractive indices of the aerogels in the counters are $n_a = 1.069 \pm 0.003$ in CkovA and $n_b = 1.112 \pm 0.004$ in CkovB. The momentum thresholds for muons pions in CkovA and CkovB are 280.5 MeV/c, 367.9 MeV/c and 217.9 MeV/c, 285.8 MeV/c, respectively [10].

The two Cherenkov detectors have been created to ensure muon purities of 99.7% in the momentum range 210 MeV/c to 365 MeV/c [15]. An expanded view of an Aerogel Cherenkov counter can be observed in Figure 2.

Cherenkov detectors utilise the Cherenkov effect in order to perform particle identification. The angle at which Cherenkov light is emitted is given by

$$\cos(\theta) = \frac{1}{n\beta}$$

where θ denotes the angle of emittance of Cherenkov light, n denotes the refractive index of the medium, $\beta = v/c$ with v being the velocity of the particle in the medium and c is the speed of light.

$\beta = 1/n$ is said to be the Cherenkov threshold. This is the minimum value of β at which Cherenkov light can be produced. The charged particle possesses a threshold energy where Cherenkov radiation is yet to be produced, that is, $\cos\theta = 1$ [17].

When $\beta > 1/n$, the charged particle has sufficient energy and velocity to produce Cherenkov light, which are emitted along the direction of the beam at an angle θ [17].

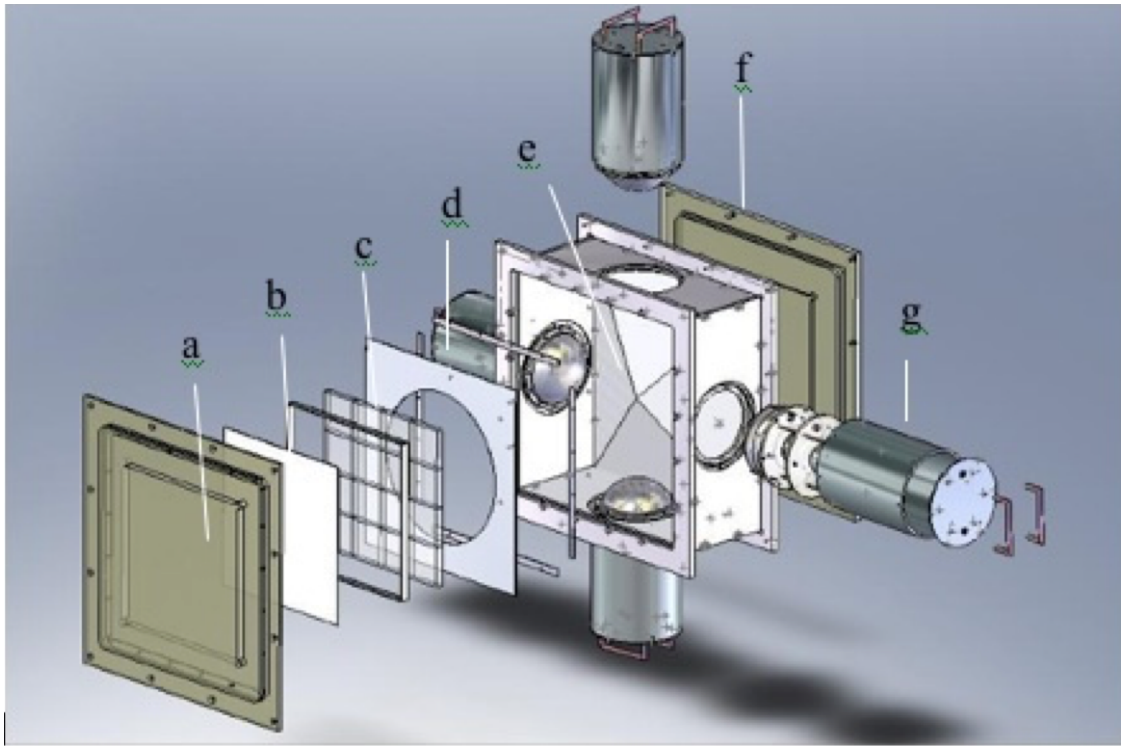

Figure 4. Aerogel Cherenkov counter blowup: a) entrance window, b) mirror, c) aerogel mosaic, d) acetate window, e) GORE reflector panel, f) exit window and g) 8 inch PMT in iron shield [16].

Due to the larger velocity of muons, they emit more photons than pions for the same momentum. Momentum of muons and pions can be obtained by the equation,

$$p = \frac{mc}{\sqrt{\frac{t^2}{t_e^2} - 1}} \tag{4}$$

where p is the momentum of the particle m is the mass of the particle, c is the speed of light in a vacuum, t is the time of flight of the particle, and t_e is the time of flight of an electron. Momentum versus Cherenkov plots can be obtained to identify the Cherenkov thresholds for muons and pions for CkovA and CkovB to conduct particle identification.

4. Results

Data was added to obtain the time-of-flight distributions as a function of momentum for each of the pion scans carried out (see Figure 5). These plots were constructed by selecting different files that include the time-of-flight data that can be converted to momentum for muons and pions (see Table 1). For each pion momentum scan distinguishable peaks in time-of-flight are observed, with varying degrees of overlap between the peaks.

Table 1. Pion momentum scans used and their corresponding μ and π momentum and Time Of Flights.

File	μ TOF (ns)	Mean μ Momentum (MeV)	π TOF (ns)	Mean π Momentum (MeV)
10488	28.0 - 31.5	166.3	34.0 - 36.0	151.3
10496	28.0 - 31.0	188.1	31.5 - 36.0	178.0
10391	27.5 - 29.0	218.9	32.0 - 36.0	202.5
10419	25.9 - 26.2	310.8	26.7 - 30.0	293.0
10304	26.0 - 27.2	322.5	27.7 - 30.0	311.3
10221	27.0 - 28.8	238.8	29.5 - 34.0	227.5
10519	25.9 - 26.2	469.6	26.7 - 30.0	420.3
07436	27.0 - 29.5	207.6	30.7 - 34.0	198.2
07437	27.0 - 28.6	229.5	29.5 - 34.0	222.4
07438	27.0 - 28.2	249.9	29.0 - 32.0	243.8
07439	26.5 - 28.0	269.9	28.8 - 32.0	257.1
07440	26.5 - 27.6	282.9	28.3 - 32.0	275.1
07441	26.5 - 27.2	306.9	28.3 - 32.0	272.6
07456	26.5 - 27.9	271.8	28.4 - 32.0	267.4
07457	26.5 - 27.6	274.3	28.6 - 32.0	263.7
07458	27.0 - 29.7	207.2	30.8 - 34.0	197.7
07459	27.0 - 28.6	229.6	29.8 - 34.0	220.6
07460	27.0 - 28.5	241.3	29.4 - 34.0	233.3

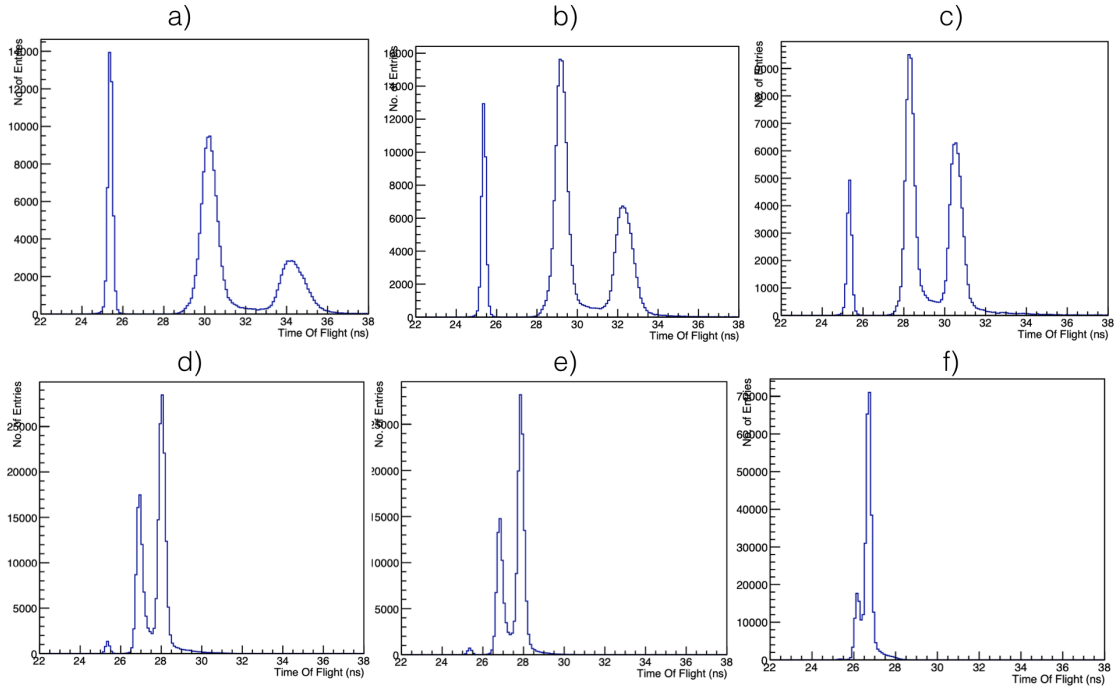

Figure 5. Time of Flight plots for a) 140 MeV muon beam b) 170 MeV muon beam c) 200 MeV muon Beam d) 240 MeV muon beam e) 300 MeV muon Beam f) 400 MeV muon beam

For pion scans in a higher momentum range, there was a noticeable contamination in the pion samples due to muons.

This contamination was minimised by making appropriate cuts in the data to separate muon and pion samples and obtain distinct time-of-flight peaks for electrons, muons, and pions. The contamination could be identified in pion time-of-flight plots by a long tail preceding the pion peak. This can be attributed to muon data entries being incorrectly identified as pions leading to a reduction in the observed momentum of pions. Furthermore, there was little data available for muons above 400 MeV which led to large error bars.

Generating the plots of number of photoelectrons (N_{PE}) as a function of momentum p (MeV) (Figure 6) confirmed that the Cherenkov threshold energy was mass dependent. Muons, having a lower mass than pions, were found to have a significantly lower energy threshold that pions. Furthermore, muons were found to emit more photons than pions for the same momentum due to the larger velocity with which muons travel.

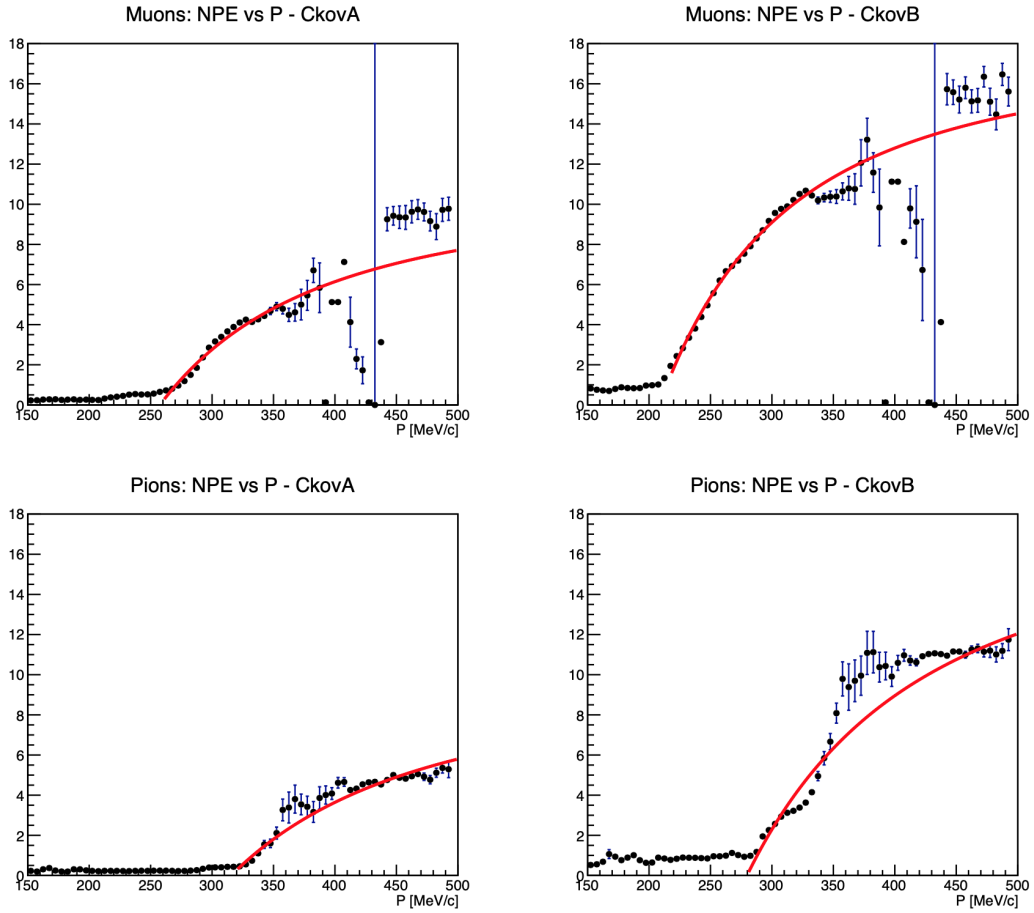

Figure 6. Momentum vs Number of photons plot for: a) Muons in CkovA, b) Muons in CkovB, c) Pions in CkovA, d) Pions in CkovB

The Cherenkov curves obtained in Figure 6 were fit with the smoothing equation,

$$N_{PE} = N_0 + N_1 \left(1 - \frac{p_0^2}{p^2}\right) \tag{5}$$

where N_{PE} is the number of photoelectrons measured, N_0 is the background noise for emitted photons, N_1 is the range for emitted photons, p_0 is the momentum threshold and p is the momentum of the bin.

Table 2. Parameters for the fits of Equation 5 to the N_{PE} vs p (MeV/c) data.

Curve	N_0	N_1	p_0 (MeV)
CkovA muons	0.28	11.58	267.16
CkovB muons	1.5	18.00	210.
CkovA pions	0.69	8.66	328.441
CkovB pions	1.31	10.61	278.69

Since

$$\cos(\theta) = \frac{1}{n\beta} <= 1$$

the Cherenkov threshold occurs when $n\beta >= 1$.

Since

$$\beta = p/E = \frac{p}{\sqrt{p^2 + m^2}}$$

the refractive index n is given by,

$$n = \sqrt{\frac{m^2}{p_o^2} + 1}$$

Using the threshold values observed in Figure 6, the refractive indices for CkovA and CkovB were found to be

$$n_a = 1.081 \pm 0.006$$

$$n_b = 1.119 \pm 0.003$$

A secondary maximum was observed in the N_{PE} vs p plot (Figure 6) for pions at CkovB. This can be attributed to significant contamination in file 10519 (Figure 7). A muon beam with a nominal momentum of 400 MeV was used in file 10519. Time-of-flight peaks observed for pions and muons were found to be overlapping. Large amount of contamination is present in the pion time-of-flight peak.

Furthermore, large error bars were observed at higher momentum. This was attributed to statistical error. The number of photoelectrons measured follow a Poisson distribution. Therefore, the uncertainty in the number of photoelectrons is given by,

$$\sigma = \frac{\sigma_{NPE}}{\sqrt{N}} \tag{6}$$

where σ is the standard deviation, σ_{NPE} is the deviation of number of photoelectrons and N is the number of events in a bin. Since the number of data entries available for larger momenta is low, the associated error in the bins was found to be high.

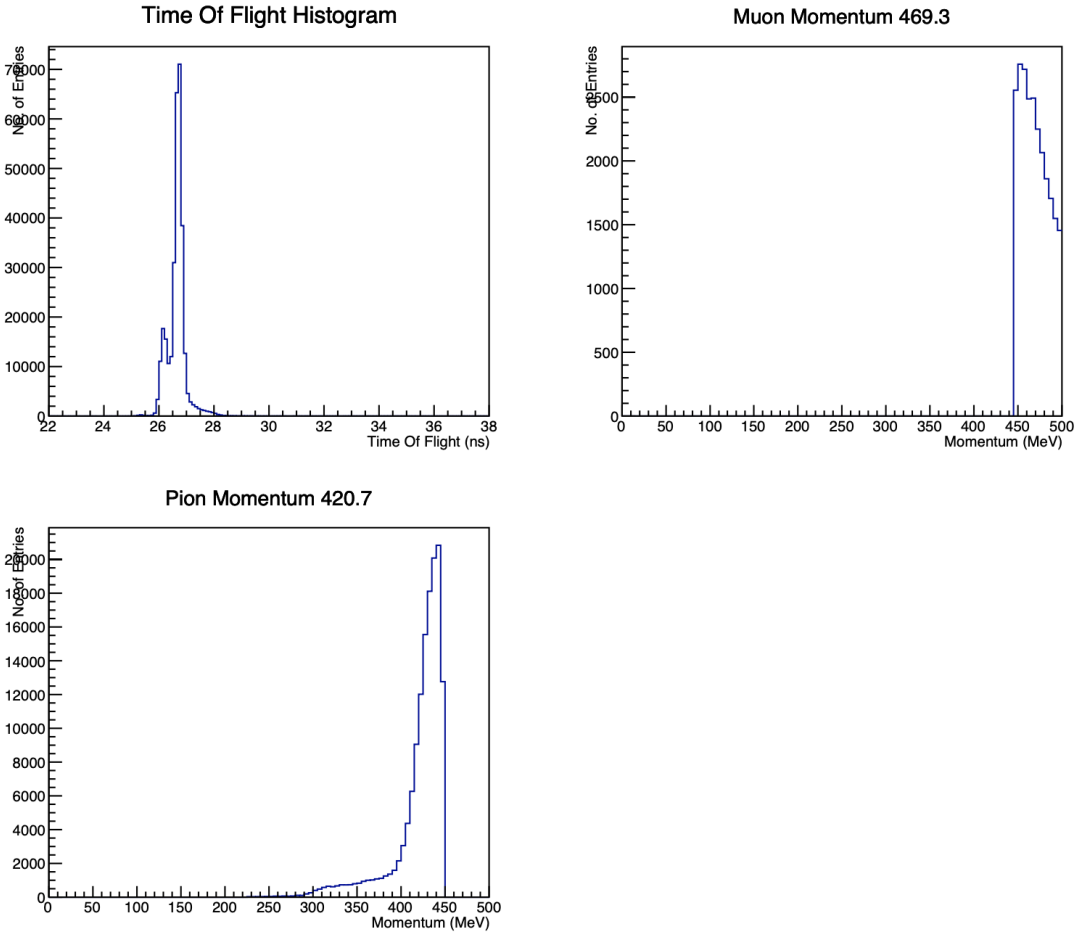

Figure 7. a)TOF plot with converging TOF peaks for 400 MeV muon beam (file 10519) b)Muon Time-Of-Flight peak c) Pion Time-Of-Flight peak with a long tail attributed to contamination arising from the muon sample.

5. Conclusion

CkovA and CkovB detectors were successfully calibrated to distinguish pions and muons. It was found that the muon Cherenkov threshold was lower than the pion Cherenkov threshold. Muons were found to emit a larger number of photons than pions did for the same momentum. Furthermore, the observed values of refractive indices for both aerogels for CkovA and CkovB were found, CkovA and CkovB, were found to be similar to the originally measured values. Significant contamination was observed in pion peaks in data procured from muon beams with a high nominal momentum. This can be mitigated by obtaining additional data for momentum above 350 MeV.

6. Bibliography

[1] Johnson R P 2007 Ionization Cooling *Beam cooling and related topics. Proceedings, Workshop, COOL 07, Bad Kreuznach, Germany, September 9-14, 2007* [Conf. Proc.C07091010,tum2i04(2007)]

[2] Bogomilov M *et al.* (MICE) 2020 *Nature* **578** 53–59 (*Preprint* `arXiv:1907.08562`)

[3] Breakthrough made on the next big step to building the world's most powerful particle accelerator `https://stfc.ukri.org/news/breakthrough-made-on-the-next-big-step-to-building-the-worlds-most-powerful-particle-accelerator/`

[4] Garisto D 2020 Mice cold: Collaboration demonstrates muon ionization cooling URL `https:`

//www.scientificamerican.com/article/mice-cold-collaboration-demonstrates-muon-ionization-cooling/
[5] Bayes R 2015 MIND at Neutrino Factories vol NUFACT2014 p 044
[6] Torun Y 2003 Mice: the international muon ionization cooling experiment *Proceedings of the 2003 Particle Accelerator Conference* vol 3 pp 1795–1797 vol.3
[7] Adams D *et al.* 2013 Characterisation of the muon beams for the muon ionisation cooling experiment (*Preprint* 1306.1509)
[8] Soler F P (MICE) 2019 Mice results vol NuFACT2018 p 015
[9] Bogomilov M *et al.* (MICE) 2012 *JINST* **7** P05009 (*Preprint* arXiv:1203.4089)
[10] Cremaldi L, Sanders D, Summers D, Drews M, Kaplan D, Rajaram D and Winter M 2015
[11] Mohayai T A 2018 First demonstration of ionization cooling in mice (*Preprint* "arXiv:1806.01807")
[12] Root reference documentation URL https://root.cern/doc/master/index.html
[13] Bogomilov M *et al.* (MICE) 2016 *JINST* **11** P03001 (*Preprint* arXiv:1511.00556)
[14] Bogomilov M (MICE) 2011 *Nucl. Phys. B Proc. Suppl.* **215** 316–318
[15] Sanders D A 2009 Mice particle identification systems (*Preprint* "arXiv:0910.1332")
[16] Bogomilov M, Karadzhov Y, Kolev D, Russinov I, Tsenov R, Vankova-Kirilova G, Wang L, Xu F Y, Zheng S X, Bertoni R and et al 2012 *Journal of Instrumentation* **7** P05009–P05009 ISSN 1748-0221 URL http://dx.doi.org/10.1088/1748-0221/7/05/P05009
[17] L'Annunziata M 2012 *Handbook of Radioactivity Analysis, 3rd Edition*